JTTEE5 3:404-411

Peel Adhesion Test for Thermal Spray Coatings

M. Sexsmith and T. Troczynski

A technique for determining the adhesion of a thermal spray coating was developed by modifying procedures commonly used to test adhesion by peeling. A coating is deposited on a metal foil that has been soldered to a massive copper block, which provides mechanical support and serves as a heat sink. Then the block, foil, and coating are glued to a stiff aluminum plate, after which the copper block is removed. The foil is peeled from the coating according to a procedure similar to the ASTM D 3167 peel test. This method causes a crack to propagate precisely along the coating/substrate interface in a stable fashion, with the movement of the crack tip controlled by the peeling speed. Sample preparation, test procedures, and initial results are discussed. The technique has been applied to testing the local variations in adhesion for plasma-sprayed Cr_2O_3 and a Ni-Mo-Al composite on a stainless steel foil. Based on these results, testing procedures are recommended and a peel test jig is specified.

1. Introduction

THE properties of thermal spray coatings often differ greatly from the properties of the bulk material, and thus characterization must take place in the as-deposited state. As coatings become more specialized, existing standard measurement techniques cease to be adequate. New standard techniques for characterizing these coatings must be developed so that deposition processes can be improved and coatings compared.

The thermal spray coating process is a violent, inhomogeneous technique and poses several problems in materials evaluation. Test samples must survive grit blasting, an extremely hot plasma flame, and the impact of hot, small, and high-velocity particles. The coating produced is far from thermodynamic equilibrium and contains complex residual stress patterns due to the rapid quenching of particles upon impact. Coatings contain many features, including microcracks, pores, impurities, in situ oxidation, and particles with a wide variety of thermal histories. The coating/substrate interface is rough, and bonding depends greatly on surface preparation and a multitude of deposition parameters (Ref 1-3).

Currently used adhesion tests are based on ASTM C 633-79 (Ref 4), which specifies a pull test in which a circular coupon is sprayed and glued to a test rod. The sample is then pulled (ideally, in pure tension) until failure. The resulting parameter is a failure stress based on the failure force and coating area. An example of a nonstandard adhesion test is a double cantilever beam (DCB) (Ref 3, 5) test where a coated beam is bonded to another beam. The crack between the beams is opened by pulling on the beam ends. The crack can be encouraged to propagate at the substrate/coating interface by the introduction of longitudinal chevron notches. From the DCB test, the fracture energy can be calculated and the process zone characterized (Ref 3). A number of other tests based on fracture mechanics have also been proposed (Ref 1). All of these tests suffer from a common problem: the location of the crack is not controlled. Thus, failure along the interface as well as through the coating or even the bonding glue is possible and is frequently observed. In order to improve control over the propagating crack and to better understand the actual interfacial toughness, a new test method is needed.

Peel testing traditionally has been used to measure the adhesion of tapes and glues (Ref 6-9). The method allows simultaneous measurement of crack-tip location and opening force. ASTM specifies several test geometries (e.g., Ref 10 and 11) that involve the peeling of a thin strip of material from a rigid substrate. These tests require that one adherend be sufficiently compliant and that, compared to the bonding energy, negligible energy be lost to bending the adherend. These assumptions work well with thin polymer strips and ductile aluminum foils, but do not apply to work-hardened or stiff materials. An energy conservation approach to approximate the energy associated with the peeling of these ideal materials has been proposed (Ref 12).

The initial reason for developing the peel test for thermal spray coatings was to study the variation in local bond strength within a coating as a function of the spray parameters and, in particular, to examine the variation of particle characteristics across the spray pattern. Variations in coating properties can be observed within a single sample (Ref 13). A simple explanation for these phenomena is that variations in the processing of different particles due to their different paths through the plasma plume are transferred to the coating due to the rastering geometry. Figure 1 shows schematically the correlation among the mass, temperature, and velocity distributions and how they combine to form regions with different properties. The original goal of the peel test was to quantify and map these variations with as high a resolution as possible, in the direction normal to the torch movement. In reality, the passes are thin and averaging

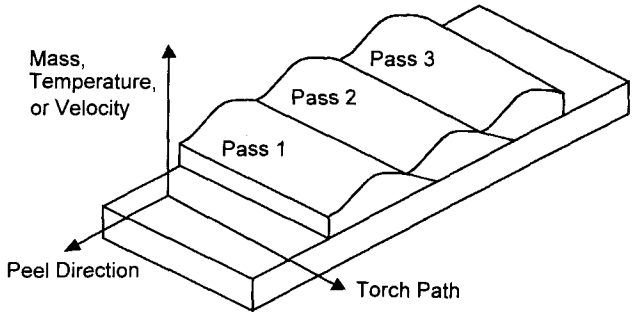

Fig. 1 Schematic of coating buildup as a superposition of passes and the geometric variation in the resulting properties

Keywords adhesion measurement, ASTM D 3167, fracture energy, peel strength, test method

M. Sexsmith and **T. Troczynski,** Metals and Materials Engineering, The University of British Columbia, Vancouver, BC V6T 1Z4, Canada.

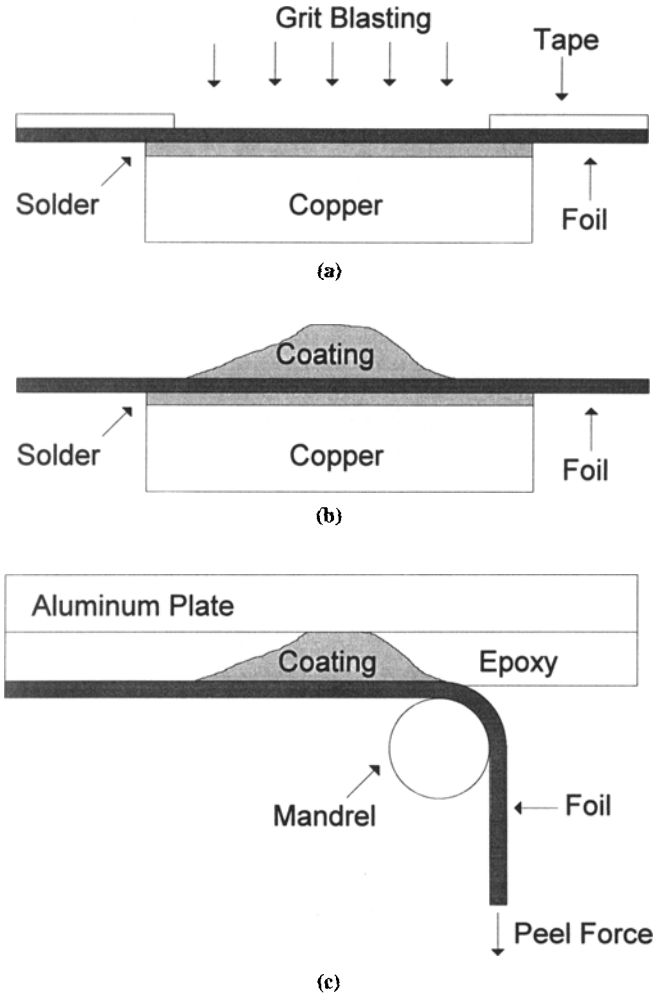

Fig. 2 (a) Schematic cross section of sample block before spraying. (b) Sample block ready for gluing to the aluminum plate. (c) Sample sandwich ready for peel testing

occurs, which tends to lessen the distribution effect. However, the bonding is affected strongly by the first set of passes and thus can be highly variable. The only truly suitable bond test to detect these variations and to link them to the process parameters is one which causes failure exactly along the interface. The use of a peel test to measure this variation was explored and found to be viable. The results discussed here relate primarily to the development of the peel test. As was expected, the colder, slower particles at the peripheries of the spray pattern showed significantly lower bond strengths than the hotter, faster particles in the center of the pattern. Details of the relationships between peel results, variations in coating properties, and spray parameters are reported elsewhere (Ref 14), and details concerning the work hardening of foils during peeling will be reported in future work.

2. Experimental

2.1 *Test Procedure*

In a peel test, a thin adherend is pulled from its substrate (in this case, a coating) with a fixed geometry, allowing the crack to propagate at the peel speed. For a homogeneous interface, the crack should experience the same stress state at each location, so that the energy required to propagate the crack is constant. The basic concept of the climbing drum test geometry (Ref 11) was chosen due to ease of implementation and jig manufacture. The test, however, is reversed in the sense that the substrate is peeled from the coating. The principal stages of sample preparation are shown in Fig. 2. A coating is deposited on a metal foil that has been soldered to a massive copper block, which provides mechanical support and serves as a heat sink (Fig. 2a and b). Then the block, foil, and coating are glued to a stiff aluminum plate, after which the copper block is removed by carefully heating the assembly to the melting point of the solder (Fig. 2c). The foil is then peeled from the coating according to a procedure similar to the ASTM D 3167 peel test (Ref 11). This method causes a crack to propagate precisely along the coating/substrate interface in a stable fashion, with the movement of the crack tip controlled by the peeling speed.

In order to adapt the peel test to thermal spray coatings, several new procedures were developed to coat and test a thin foil. Both foil chemistry and peeling geometry were considered to be important factors in the test. A small process zone is needed to ensure controlled crack propagation along the interface. This prevents long-range effects that might cause the crack to deviate from the interface into the coating (Ref 3). A small-radius mandrel (6.35 mm in diameter) was thus utilized to maximize foil strain at the interface within a small, well-defined region. A small mandrel also causes the crack tip to be precisely located. A thin, hot-corrosion-resistant adherend that matches the chemistry of common substrates was required. Accordingly, the test procedure described here has evolved to meet the demands of the toughest testing situation, where a brittle, high-melting-point ceramic coating is applied to a work-hardening foil. The test can thus be performed on less extreme systems, such as a metallic coating on a compliant foil, without much difficulty.

The thin foil test substrate should behave like the bulk substrate. Most ceramic coatings are sprayed on either steels or cast alloys. Usually, a corrosion-resistant bond coat is applied to materials prone to high-temperature oxidation. These bond coats typically are Ni-Cr-Mo or Ni-Cr-Al alloys. In order to mimic the general chemical properties of these bond coats and substrates, a stainless steel foil (Fe-17.5Cr-7Ni-2.2Si-2Al-1.5Mn) was chosen as a substrate in this work. This type of foil is readily available in a variety of thicknesses as shim stock. The possibility of using a more ductile nickel foil as well as other materials also was explored, and the results will be reported at a later date. Stainless steel is a work-hardening material, and thus the plastic work consumed to bend it to the mandrel must be included in calculations of peel strength. A 75 μm (0.003 in.) stainless steel foil was the easiest substrate material to work with, although with careful handling a 38 μm (0.0015 in.) foil could be used. The thinner foil gives a smaller process zone, and less plastic work is consumed in bending it to the mandrel.

In order to provide mechanical backing and a thermal sink, the foil was soldered to a copper block (Fig. 2a). This was accomplished by coating the foil with 60Sn-40Pb solder using an electric soldering iron and a rosin flux. A copper block was also coated with the solder using a propane torch. The foil and solder were both cleaned and then clamped together. The entire assem-

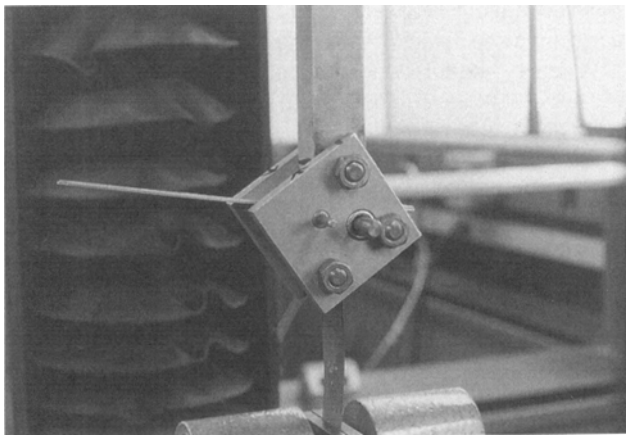

Fig. 3 Test jig as mounted in testing machine. A sample is threaded through the rollers and clamped in the lower jaw.

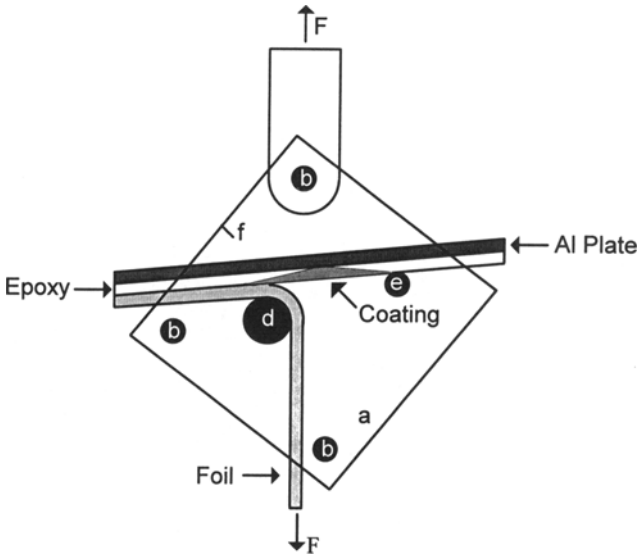

Fig. 4 Schematic of test jig showing the threading of the foil through the rollers and the applied forces. Under normal test conditions, the foil would conform exactly to roller d.

bly was heated with the propane torch until solder flowed from the joint. The clamps were retightened and the assembly allowed to cool. Figure 2(a) shows a schematic of the prepared samples. The samples were then cleaned and degreased, and tape was used to mask all but a rectangular area (50 by 20 mm) on the foil. This area was grit blasted with 60-grit Al_2O_3 at 100 psi. Care was taken to grit blast each sample in an identical fashion. The masking was removed and the samples cleaned with dry compressed air.

The samples were mounted in the spray booth and coated. Because the variation in adhesion versus torch axis was of interest, the plasma torch was rastered in only one direction. This provided a coating profile with different properties across its section (Fig. 2b). An axial feed torch (Northwest Mettech Axial III, Richmond, BC, Canada) was used to spray samples with PraxAir 117 Cr_2O_3 using parameters developed in-house. A radial feed torch, Metco MBN (Metco Perkin Elmer, Westbury, NY) was used to spray both a Ni-Al-Mo composite (Metco 447) (Metco Perkin Elmer, Westbury, NY) and Cr_2O_3-silica (Metco 136F) (Metco Perkin Elmer, Westbury, NY) using the manufacturer's suggested spray parameters. The sprayed samples were cleaned with alcohol and were then glued, using Master Bond EP 15 (Master Bond, Inc., Hackensack, NJ) thermoset epoxy, to a clean, grit-blasted, 1 mm thick aluminum plate. After the glue cured, the samples were placed on an electric hot plate until the solder melted. The aluminum, glue, coating, and foil sandwich were separated from the copper block (Fig. 2c), and the melted solder was quickly brushed off the foil using steel wool. The edges of the sandwich were ground parallel on a wet SiC wheel, thus eliminating the possibility of edge effects. Grinding with successively smaller grits minimized the size of the damage zone. The sandwich was allowed to dry before being threaded through the test jig.

Figure 3 shows the test jig mounted in an Instron (Instron Corporation, Canton, MA) universal testing machine. The jig is similar to the standard (Ref 11), but has a narrower sample width and smaller mandrels. Details of the jig are discussed in Section 2.2. The sample was mounted in the jig as shown in Fig. 3 and 4, and the starting tab was clamped into the jaw. The foil was pulled from the coating at a constant rate of 2.5 mm/min. The load and crosshead displacement were monitored and recorded digitally. Examples of the generated curves are shown in Fig. 6 (which will be discussed in Section 3). The test repeatability is excellent for different samples of the same coating.

The effects of crosshead displacement rate on peel force were explored within the range of 25 to 0.25 mm/min. High peeling rates cause the measurement of higher peel loads, which suggests some frictional effects. The standard test speed of 2.5 mm/min was selected by lowering the speed while peeling the same coating until further speed reductions had no effect on measured load.

2.2 *Details of Test Jig*

The test jig is based on the climbing drum system recommended by ASTM D 3167 (Ref 11). As shown in Fig. 4, two parallel plates (a) are held 20 mm apart by three fixed studs (b). The top stud acts as a pivot for the pull bar (c). This centers the line of action of the peel force through the center of the stud. Two mandrels are arranged so that peeling can be performed around either one. One mandrel (d) is 6.35 mm (0.25 in.) in diameter and the other (e) is 3.175 mm (0.125 in.). They are set in needle roller bearings that have been press fit into the plates. Two mandrel sizes were used so that the effects of bend radius could be explored. The mandrels are removable to allow threading of the foil. As shown in Fig. 4, the line of action of the forces is between the center of the top stud to the outside edge of the mandrel. The rotational freedom of the jig allows the system to align itself. The geometry is such that the sandwich is always climbing slightly during the test. This prevents the specimen assembly from sliding along the rollers. The elastic component of the bending of the foil would sometimes cause the sandwich to lift from the mandrel, as shown in Fig. 4. This occurred only for weak bonds on the large mandrel, but occurred regularly on the smaller mandrel. The effect was also dependent on peel speed. Faster peel rates caused the foil to conform better to the mandrel.

A second-generation jig has been designed to eliminate the problem. In the new jig, both mandrels are 6.35 mm (0.25 in.) in diameter and are symmetrically spaced. A third spring-loaded roller is used to push the sandwich onto the peeling mandrel, adding to the compressive stresses in front of the crack and forcing the foil to conform to the mandrel. The use of a thinner or more ductile foil would also reduce the problem. It should be noted that the riding effect was stable and that repeatable but noisier results were found even if the problem occurred (e.g., compare Fig. 6b and c). This aspect is discussed in Section 3.

The jig forces the crack tip to stabilize because the reaction force from the roller causes a compression stress field in the sandwich in front of the crack tip. Several tests were performed to determine the crack-tip location relative to a mark (f) on the jig (see Fig. 4). This was accomplished by stopping a peel test and marking the sandwich adjacent to the jig mark. The sandwich was then removed from the jig and the distance measured from the crack tip to the mark. The results were repeatable within 0.3 mm. This calibration allows identification of the location of the crack-tip position relative to a fixed specimen origin.

2.3 *Test Interpretation*

In order to quantify adhesion in a peel test, a conservation-of-energy equation can be written for constant-velocity peeling. This is a stable state of the system and is reached after about 10 mm of peeling the starting tab. The incremental energy input to the system (U_{tot}) comes only from the peel force (F) and the displacement of the end of the foil (dx):

$$U_{tot} = F \cdot dx = U_{crack} + U_{plastic} + U_{friction} \quad \text{(Eq 1)}$$

where U_{crack} is the energy to open the coating/substrate interface, $U_{plastic}$ is the energy dissipated in bending the foil, and $U_{friction}$ is the energy lost to jig friction, all in joules. It should be noted that the plastic work in the coating material and in the foil which is not part of the macroscopic bending is included in the crack-opening energy term because this work is required to propagate a crack through the interface. In this derivation, it is assumed that frictional effects in the jig ($U_{friction}$) are negligible if small peel velocities are used. To propagate a crack of width w, along an interface with adhesion R, a distance dx, the energy is given by:

$$U_{crack} = R \cdot w \cdot dx \quad \text{(Eq 2)}$$

According to Eq 1 and 2, for a constant foil thickness and sample width, the instantaneous value of R is given by:

$$R = \frac{F}{W} - \frac{U_{plastic}}{w \cdot dx} \quad \text{(Eq 3)}$$

According to Eq 3, in order to determine peel adhesion R, the measured peel force is divided by the sample width, which gives a result in newtons per meter (N/m) or joules per square meter (J/m^2). The amount of plastic work ($U_{plastic}$) per unit width is subtracted from the peel force, giving the instantaneous energy per unit width required to separate the foil from the coating, defined here as the peel strength. The value of $U_{plastic}$ for a work-hardening foil has been evaluated by integrating the stress versus strain curve for all the strained elements over the strains

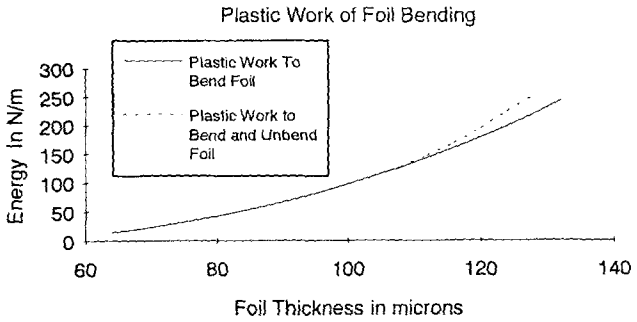

Fig. 5 Plot of the work to bend a stainless steel foil to a mandrel with a radius of 6.25 mm for various foil thicknesses. The "bending only" (solid) curve represents the plastic work required to bend a foil to the mandrel. The "bending and unbending" (dashed) curve represents the plastic work required to both bend and unbend a foil.

experienced by each element. The derivation of the necessary expressions will be the subject of a future paper. The results of a sample calculation for $U_{plastic}$ are shown in Fig. 5. The calculation is for a fully hardened foil where very little plastic work is done. For some samples the foil was annealed, causing much higher amounts of plastic work. With the foils used in this study, the plastic work was between 30 and 200 N/m. Errors associated with this procedure will affect only the position of zero peel strength on the scale, and thus the magnitude of variation remains unaffected. If the same foil is used for all tests, then the error will affect all tests equally.

Although the units are identical, the relationship between peel strength and interfacial fracture toughness is difficult to define. From a microscopic viewpoint, the interface between two materials is a complex region in which van der Waals forces, mechanical interlocking, and interdiffusion combine to form a bond. The interface is not defined easily as a surface, but should be considered to be a three-dimensional region across which the physical material properties change. A propagating crack finds the easiest path through this region under the constraints of the test arrangement. This path will depend as much on the local stress state as it does on the locally varying material properties. The roughness of the interface causes widely varying local stress states. The results of the peel test thus should not be considered a measure of the interfacial fracture toughness. Therefore, the results are reported in newtons per meter (N/m) and defined as a peel strength. This conforms to the format specified by ASTM D 3167 . Some researchers (Ref 6, 7, 15) have attempted to relate the results of the peel test to fracture mechanics concepts, but further work is needed to establish any useful relationships for the unique case of thermal spray coatings.

3. Results

The initial results of the peel tests are shown in Fig. 6. In each test, two sample strips were peeled from the same coating and the two resulting curves plotted. Although the curves are corrected for the constant effect of plastic work (except Fig. 6b), the amount of data manipulation is minimal. The data sampling system reports the average of 10 force samples over a peel distance of 69 μm, and the curves are generated by connecting the data points. Because this average is of the same order of magnitude

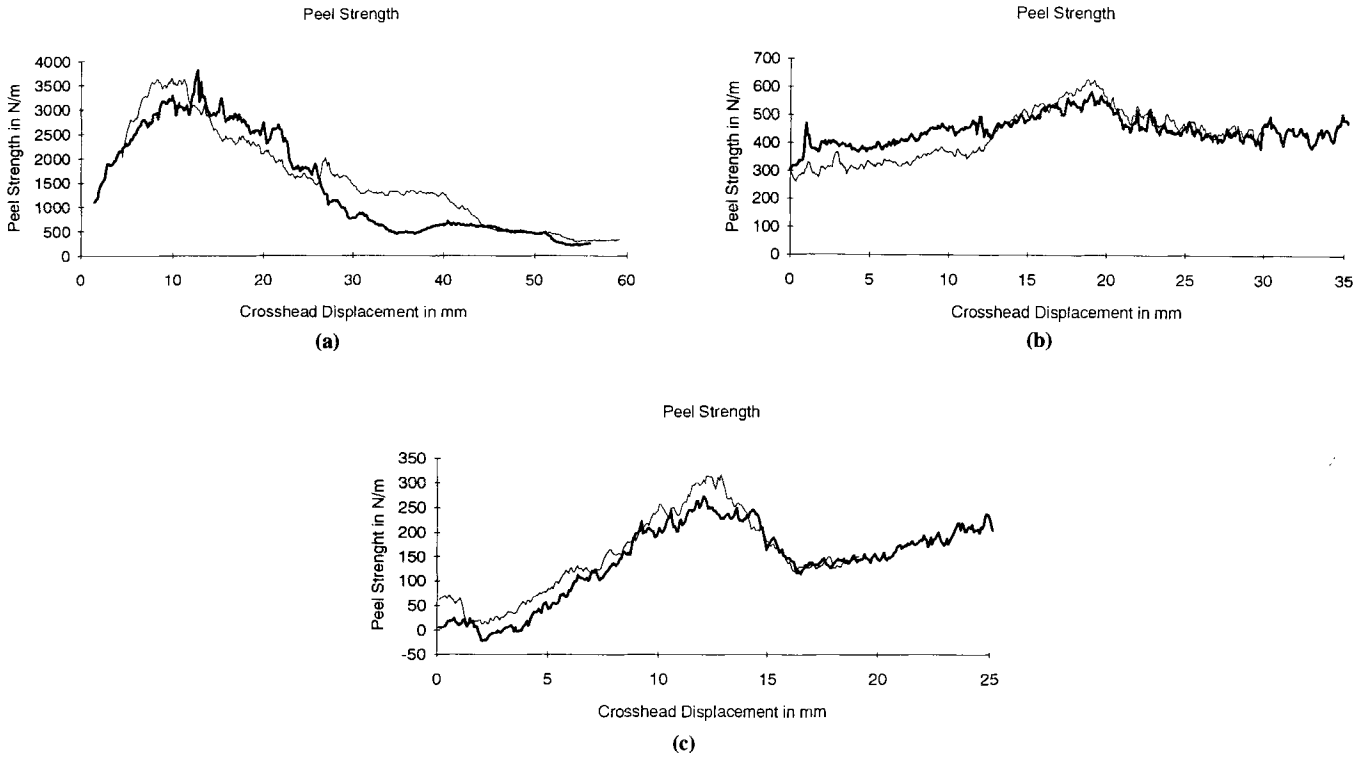

Fig. 6 Peel strength curves. (a) Ni-Al-Mo composite with radial feed. (b) Cr-Cr_2O_3 coating with axial feed. (c) Cr_2O_3-silica coating with radial feed. Two tests are indicated on each graph.

as the diameters of the particles sprayed, the test resolution is close to the size of individual particles averaged over the strip width (18 mm).

The curves indicate that the test is a valid measurement of the variation of the bond strength of the coatings. A large repeatable variation across each sample was observed. The shape of each curve shows the same symmetries as curves describing the variation in particle velocity and temperature within the plasma plume (Ref 16). The results were equally valid for the metal and ceramic coatings. The variations measured are easily observed in the raw data and are readily separated from the plastic work in the foil.

3.1 *Specific Tests*

Figure 6(a) shows the variation in bond strength across a profile sample of a Ni-Al-Mo composite powder sprayed with a radial feed torch on an annealed unsoldered foil (76 μm thick). This test was undertaken to determine whether soldering the foil to a heat sink was necessary. The foil was held to a block by clamping it at both ends. During spraying, thermal gradients caused the foil to kink and warp. As can be seen in Fig. 6(a), the profile between two samples was repeatable despite the kinking problem. Many of the large spikes on the curve correspond to individual kinks in the foil where nonuniform peeling occurred. This test indicated that soldering was necessary to ensure heat transfer away from the foil and that peel strength variations are relatively easy to measure.

The peel strength curve exhibits a distinctive nonsymmetry. The nonsymmetric distribution of mass, momentum, and temperature in a radial feed plasma plume is quoted in the literature (Ref 16). Use of the peel test enables the combined effect of these skewed distributions on the level of local adhesion to be shown. The peel strength changes by a factor of seven between the peak where the "best" particles arrived and the periphery where the coldest, slowest particles arrived.

Figure 6(b) shows the peel strength for a profile of a Cr-Cr_2O_3 coating sprayed with an axial feed torch. It was sprayed on a thicker (127 μm), less compliant foil than the other samples and was thus capable of storing more elastic energy. During peeling the sample did not totally conform to the mandrel (point d in Fig. 4); as a result, the curve cannot be properly corrected for plastic work. The constant amount of plastic work would need to be subtracted from the curve, which would uniformly shift the position of zero peel strength on the scale. The curve appears noisy due to the instability introduced by the large amount of elastic energy stored in the system. Again, despite the problem with this test, a repeatable measurement of the adhesion variation was obtained. The sample showed the limitations associated with using thick foils. The test also showed that the axial feed torch produces a symmetrical peel strength curve.

Figure 6(c) shows the variation in adhesion across a profile of a Cr_2O_3-silica coating sprayed with a radial feed torch. The zero position indicates the centerline of the torch, and the arrow indicates the feed direction. Traces from both samples show a clear repeatable variation in adhesion across the sample, which can be explained in terms of the spray profile characteristics. The bond strength drops to zero at the far edge of the profile, where the coldest and slowest particles arrived. This indicates that, al-

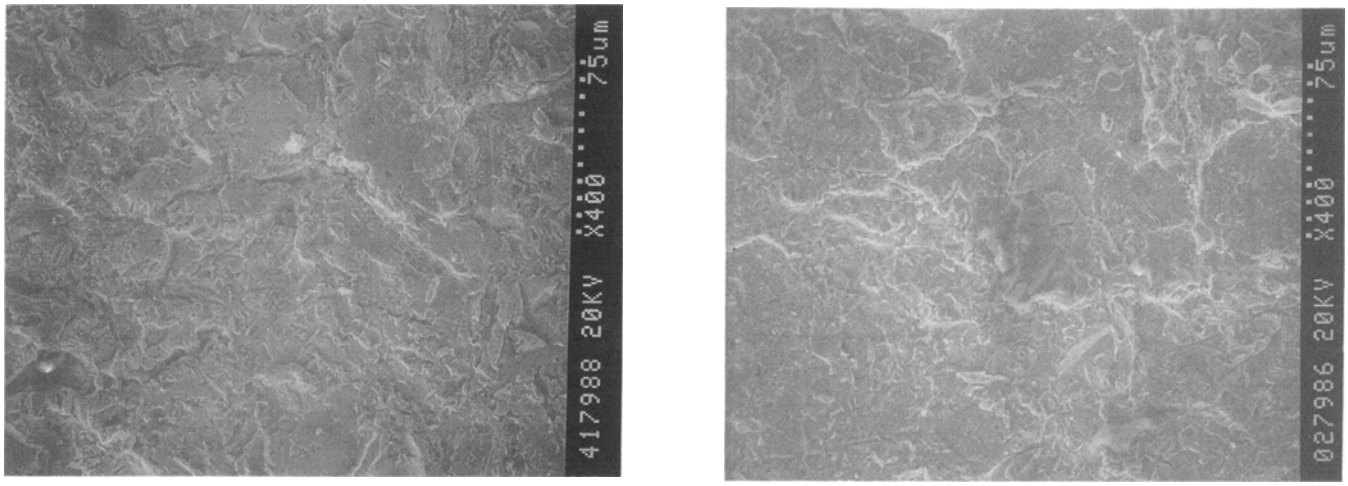

(a) (b)

Fig. 7 Scanning electron micrographs of failures of the same foil surface. (a) Just before coating. (b) Just after peeling. Note that no residue from the coating is found on the surface shown in (b), although some debris is present from handling. Both 400×

though the particles did stick to the substrate, the bond was extremely weak. The highest bond strength occurs at a position offset from the torch centerline. This position is close to the thickest point on the coating, indicating that the majority of the particles were processed to give good bonding. On either side of the profile, the bond strength rises gradually to that of the adhesive used to bond the coating to the rigid aluminum plate. This occurs in a region where the coating is sufficiently thin that the adhesive can penetrate and bond to the substrate. It is possible that the properties of these poorly processed spray pattern peripheries are locked into the coating by subsequent passes and remain as flaws in the coating. The large dip near the center of the top curve corresponds to a defect observed on the peel surface where the crack propagated into the coating and left some coating bonded to the foil. This is a rather rare defect in the peel test, which confirms that the state of stress ahead of the crack tip encourages separation along the interface.

3.2 *Signal Variations*

Signal noise was observed on top of the main variation of the peel strength. The test apparatus could be expected to generate variations of 2%. Larger variations must be considered significant, although no clear relationship exists between these variations and the crack propagation characteristics or microstructural features of the coating, substrate, or interface. However, a degree of repeatability in both amplitude and apparent frequency of the noise for two similar samples suggests some type of relationship. The noise is possibly indicative of a slip-stick type of crack propagation, or it may reflect the variation in bond strength on a small scale. Fourier analysis showed no pattern to the noise at frequencies below the sampling frequency, which indicates that the cause of the noise is random in nature. The small wavelength of the noise signal indicates the degree of stability. The crack can propagate only a short distance before the stresses drop below the level required to continue cracking. The small noise amplitude allows the observation of relatively small variations in adhesion. Many of the larger noise events can be related to features on the peeled surface. Although the crack normally propagates along the interface, small deviations into the coating and farther into the glue occur. Defects in the foil created during sample preparation can cause local overheating of the foil. These features promote local changes in bond strength. The relationship between the small-scale peel strength variations and the mechanics of the cracking system will be the subject of further study.

4. Discussion

The peel strengths are up to 300 N/m for the ceramic coating and are an order of magnitude higher for the metallic coating. A high-performance adhesive would have a peel strength of 5000 N/m. Fractography indicates that all surfaces separated exactly at the interface, with only minor observable exceptions. Figure 7 shows scanning electron micrographs of the foil before coating and after peeling. No significant coating residue was found on the peeled foil. As previously mentioned, plasma spray coatings are applied to grit-blasted surfaces and thus the true area of contact is much greater than the measured sample size (Ref 17). The true area is affected by the foil properties and the grit-blasting procedure. The increase in contact area does not entirely explain the high peel strength values. Figure 8 schematically shows some of the possible energy-dissipation mechanisms that might cause the high peel strength. These include friction between asperities, local plastic work within asperities, and microcracking in the coating. Investigation of these mechanisms is difficult because both local plastic work and microcracks exist in the system prior to peeling. Detection of changes in the amount of plastic work and degree of microcracking require further investigation. The quantification of friction is equally difficult. Therefore, it is not yet possible to calculate an intrinsic interfacial energy for thermal spray coatings with this method. However, the measured value of peel strength can be compared

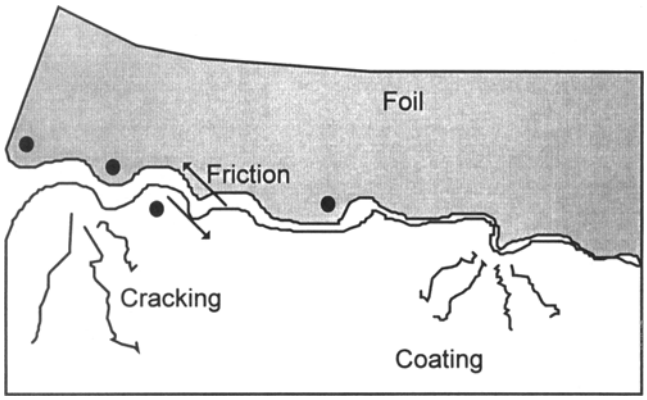

Fig. 8 Expanded view of coating substrate interface showing possible mechanisms of energy dissipation during cracking

with other materials measured in the same manner. This makes the test useful for understanding the variation in bonding within a sample. If a standard substrate is used, the method allows the comparison of different coatings. Thus, the technique can be used for quality control and process optimization in a much more informative and reliable way than existing tests.

The question of why the crack propagates along the interface and not some other lower-energy path, such as through the coating, is difficult to answer. The special geometry of the test is the likely cause. Because of the small mandrel size, high foil strains are concentrated in a small region. The difference in the ability of the materials on each side of the interface to accommodate strain causes the stress field to be concentrated close to the interface. Models of the peel test (Ref 6, 7) indicate that the geometry forces the crack to propagate along the interface. The crack follows the local lowest-energy path, which is the interface. In this case the "extra" toughness may come from the mechanisms described previously that occur due to the rapidly increasing strains behind the crack tip. This explanation is overly simple, and a better understanding of crack propagation along highly strained rough interfaces is necessary. The experimental data indicate, however, that high energies are measured and that failure occurs exactly at the interface. This is considered the greatest advantage of using the peel adhesion test to evaluate thermal spray coatings.

5. Conclusions

The results of these initial tests indicate that the peel test is a good method for measuring the adhesion of thermal spray coatings. The climbing drum peel test, in which a stainless steel foil is peeled from a thermal spray coating around a drum, is both easy and inexpensive to perform. By directly measuring the force required to peel the foil, the variations in adhesion across the sample are easily calculated. Repeatable measurements of the variations in adhesion within a coating were achieved, thus allowing the test to be used for coating evaluation and comparison. The observed details of the variations may lead to a better understanding of the mechanism of failure along the coating/substrate interface. The preparation of foil samples is simple, requiring only common tools and materials. The test itself requires little special equipment and thus can be performed without great expense (the highest cost involving the actual spraying). The peel test is a long-established method for testing adhesives, and the results of this test conform to the format used when testing adhesives. This allows the results to be related to recent work (Ref 8, 18, 19, 20) on the fundamental aspects of adhesion.

Further work is required to fully characterize the test. This includes testing of a wider variety of coatings using vacuum plasma spraying, high-velocity oxyfuel spraying, and atmospheric plasma spraying. The test results should be compared to tensile pull tests and ultrasound interfacial integrity tests (Ref 21). A more detailed model of the meaning of the measured peel strength in terms of energy should be formulated that accounts for roughness and microcracking in the coating. Foils of a wide variety of compositions and thicknesses should be studied, as should the relationship between peel speed and peel load. However, even without such future work, the test can be used to characterize and compare thermal spray coatings to improve processing parameters. This new work allows comparisons to be made to other adhesion systems and to the predictions of fracture mechanics.

References

1. S. Brown, B. Chapman, and G. Wirtz, Fracture Kinetics and the Mechanical Measurement of Adherence, *Thermal Spray Technology—New Ideas and Processes*, D.L. Houck, Ed., ASM International, 1989, p 147-157
2. H.S. Ingham, Jr., Adhesion of Flame Sprayed Coatings, in *Adhesion Measurement of Thin Films, Thick Films and Bulk Coatings*, K.L. Mittal, Ed., ASTM, 1976, p 285-291
3. T. Troczynski and J. Camire, "Resistance to Fracture of Thermal Sprayed Ceramic Coatings," The University of British Columbia, Vancouver, 1994
4. "Standard Method of Test for Adhesion or Cohesive Strength of Flame Sprayed Coatings," C 633-79, *Annual Book of ASTM Standards*, ASTM
5. C.C. Berndt and R. McPherson, The Adhesion of Plasma Sprayed Ceramic Coatings to Metals, *Mater. Sci. Res.*, Vol 14, 1981, p 618-628
6. R. Adams, A. Crocombe, and J. Harris, The Mechanics of Peel, *Adhesion 7*, K. Allen, Ed., Elsevier Applied Science, London, 1983, p 39-58
7. A. Crocombe and R. Adams, Peel Analysis Using the Finite Element Method, *J. Adhes.*, Vol 12, 1981, p 127-139
8. R. Adams, Testing of Adhesives–Useful or Not, *Adhesion 15*, K.W Allen, Ed., Elsevier Applied Science, London, 1991, p 1-17
9. J. Rice, Adhesive Selection and Screening Testing, *Handbook of Adhesives*, I. Skiest, Ed., Van Nostrand Reinhold, 1990, p 94-115
10. "Standard Test Method for Peel or Stripping Strength of Adhesive Bonds," D 903-49, *Annual Book of ASTM Standards*, ASTM, 1983
11. "Standard Test Method for Floating Roller Peel Resistance of Adhesives," D 3167-76, *Annual Book of ASTM Standards*, 1986
12. A. Atkins and Y. Mai, *Elastic and Plastic Fracture*, Ellis Horwood Ltd., 1985, p 289-296
13. E.H. Lutz, Plasma Ceramics, *Powder Metall. Int.*, Vol 25, 1993, p 131-137
14. M. Sexsmith and T. Troczynski, "Variations in Coating Properties across a Spray Pattern," University of British Columbia, 1994
15. M.D. Thoules and H.M. Jensen, Elastic Fracture Mechanics of the Peel Test Geometry, *J. Adhes.*, Vol 38, 1992, p 185-197
16. J.R. Finke and W.D. Swank, Simultaneous Measurement of Ni-Al Particle Size, Velocity, and Temperature in Atmospheric Thermal Plasmas,

Thermal Spray: International Advances in Coating Technology, C.C. Berndt, Ed., ASM International, 1992, p 39-43

17. F. Tzschichholz and M. Pfuff, Influence of Crack Path Roughness on Crack Resistance in Brittle Materials, *Fracture Processes in Concrete, Rock, and Ceramics*, J.G.M. van Mier, Ed., E&F.N Spon, London, 1991, p 251-259
18. W. Brockman, Some Analytical and Theoretical Aspects in Adhesion Science, *J. Adhes.*, Vol 37, 1992, p 173-179
19. L. H. Lee, Molecular Bonding Mechanism for Solid Adhesion, *J. Adhes.*, Vol 37, 1992, p 187-204
20. S. Kuroda, T. Fukushima, and S. Kitahara, Significance of the Quenching Stress in the Cohesion and Adhesion of Thermally Sprayed Coatings, *Thermal Spray: International Advances in Coating Technology*, C.C. Berndt, Ed., ASM International, 1992, p 903-909
21. Y. Suga, Harjanto, and J. Takahashi, Study on the Ultrasonic Test for Evaluating the Adhesion of Thermal Sprayed Coatings to a Substrate, *Thermal Spray: International Advances in Coating Technology*, C.C. Berndt, Ed., ASM International, 1992, p 247-252